Polish Journal of Chemical Technology, 19, 2, 6—15, 10.1515/pjct-2017-0021

Novel lignocellulosic wastes for comparative adsorption of Cr(VI): equilibrium kinetics and thermodynamic studies

Hajira Haroon[1, 3], Syed Mubashar Hussain Gardazi[1], Tayyab Ashfaq Butt[2], Arshid Pervez[1], Qaisar Mahmood[1], Muhammad Bilal[1*]

[1]*COMSATS Institute of Information Technology, Department of Environmental Science, Abbottabad, 22060, KPK, Pakistan*
[2]*University of Hail, Department of Civil Engineering, Hail Province, Saudi Arabia*
[3]*University of Haripur, Department of Environmental Sciences, 22620, KPK, Pakistan*
[*]*Corresponding author: e-mail: mbilal@ciit.net.pk*

Cr(VI) adsorption was studied for abundantly available low-cost lignocellulosic adsorbents in Pakistan namely, tobacco stalks (TS), white cedar stem (WCS) and eucalyptus bark (EB). Several process variables like contact time, adsorbent dose, pH, metal concentration, particle size and temperature were optimized in batch mode. EB showed high Cr(VI) adsorption of 63.66% followed by WCS 62% and TS 57% at pH 2, which is higher than most of the reported literature. Langmuir isotherm (R^2 = 0.999) was well fitted into the equilibrium Cr(VI) data of EB, suggesting homogeneous active sites and monolayer coverage of Cr(VI) onto the EB surface. Freundlich (R^2 = 0.9982) isotherm was better fitted to the equilibrium data of TS and WCS, revealing the adsorption sites with heterogeneous energy distribution and multilayer Cr(VI) adsorption. Moreover, the Cr(VI) adsorption of studied adsorbents followed the pseudo-second order kinetic model. Thermodynamic properties were investigated in two temperature ranges, i.e., T_1 (303–313 K) and T_2 (313–323 K). TS and EB showed the exothermic at T_1 and endothermic reactions at T_2 with entropy controlled adsorption at the solid-liquid interface, and WCS exhibited an opposite thermal trend with decreasing disorderness at solid-liquid interface as temperature rises. Gibbs free energy ($\Delta G>0$) confirmed the non-spontaneous adsorption process for all studied adsorbents.

Keywords: chromium VI, equilibrium kinetics, lignocellulosic waste adsorbents, thermodynamics.

INTRODUCTION

Cr(VI) is classified as one of the top main alarming noxious pollutant (US, EPA). It is released from industrial effluents like chromic salts industry, electroplating, alloying, textile dyeing, leather tanning, metal polishing and pigment manufacture. 40% unused chromium salts are released in the final effluents during the process of chrome tanning and causes a serious environmental risk[1]. The tolerable limits for Cr(VI) in drinking and inland waters, set by World Health Organization (WHO) and US EPA, are 0.05 mg L^{-1} and 0.1 mg L^{-1}, respectively. In natural water, chromium exists mainly in two stable oxidation states, hexavalent chromium (Cr(VI)) and trivalent chromium (Cr(III)), as other oxidation states of chromium are unstable in aqueous solution[2]. However, Cr(VI) has high mobility, solubility in water and oxidizing power, which makes it 100 fold more toxic than trivalent chromium and remain bioavailable for 39 hours within the body[3]. Cr(VI) can act as carcinogen, teratogen, and mutagen in biological systems[4].

Numerous treatment methods have been applied to remove Cr(VI) from wastewater, for instance, ion exchange, electrodialysis, solvent extraction, reverse osmosis[5], membrane filtration, ultra filtration, microfiltration[6], catalytic oxidation[7] and biological operations[8]. Economic and disposal issues make these methods environmental unfriendly, because of the consumption of acid and alkali, sludge production, pH constraints in ion exchange, toxic solvent loss, membrane fouling and high cost[9–11]. The commercially available adsorbents (usually activated carbon) are also costly and thus, can't be practiced at industrial-scale application. Therefore, the development of cheap, efficient and abundantly available waste alternatives yet needs to be explored for Cr(VI) adsorption.

Adsorption is a simple, easy and low-cost process, used for Cr(VI) removal from wastewater. Different biomasses, like tea waste[12], neem leaves[13], potato peelings[14], rice straw[15], *Pinus roxburgii* bark[16], Bengal gram husk[17] and maize corn cob[18] have been used for adsorption of Cr(VI). Two main factors involved in the successful metal uptake by agricultural wastes are the chemical composition of lignocellulosic biomass, and acidic functional groups, e.g., carboxylic and phenolic groups on the biomass surface. These groups can form complexes with heavy metals by hydrogen ion's replacement or through an electron pair donation from these groups.

Pakistan is major producer of tobacco, which is higher than China, India, Brazil, America and Greece. The total area reported for tobacco cultivation is 0.037 million hectares with the production of 0.088 million tons in KPK province only. After harvesting of leaves, stalks are mostly left in the cultivated land as waste. Eucalyptus was introduced in Pakistan from Australia as a solution to water logging and soil erosion. This tree has been widely planted in watershed area of Tarbela dam, Pakistan. Its bark is peeled out every year. Moreover, white cedar is a common tree found in all four provinces of Pakistan and is famous for furniture and fuel wood. Therefore, these low-cost lignocellulosic wastes biomasses namely; tobacco stalks (TS), eucalyptus bark (EB) and white cedar sawdust (WCS) were explored for their Cr(VI) adsorption potential from the aqueous solution in a batch system. Moreover, adsorption isotherms, kinetics and thermodynamic studies were carried out to find adsorption mechanisms.

EXPERIMENTAL

Chemicals and reagents

1000 ppm stock solution of potassium dichromate ($K_2Cr_2O_7$) was prepared. Furthermore, dilutions were carried out to get the solutions with required concentrations. 0.1 mol L^{-1} NaOH or 0.1 mol L^{-1} H_2SO_4 were used for the pH adjustment of the solutions.

Preparation of adsorbent

Lignocellulosic waste adsorbents, namely maize cob (MC), sisal leaves (SL), peanut shells (PS), tobacco stalks (TS), white cedar stem (WCS) and *eucalyptus* bark (EB) were collected from KPK province, Pakistan. These biomasses were washed with deionized water to remove any dust particles, and afterwards, dried at room temperature. All the dried adsorbents were ground, and analytical sieves were used to acquire the various particle sizes (104–420 μm). The adsorbents were kept in a desiccator prior their usage in batch experiments.

Batch adsorption experiments

In the batch experiments, 0.05 g of adsorbent dose was added to the 50 mL Cr(VI) solution in 100 mL flask, and agitated in a temperature controlled orbital (220 rpm) shaking incubator (Wise Cube, Korea) at 30°C. The samples were taken out from the shaker at already determined time intervals. After centrifugation at 4000 rpm for 5 minutes, the supernatant was collected using filter paper of 0.45 μm size. Cr(VI) in the filtrate was analyzed by atomic absorption spectrophotometer (AA 700, Perkin Elmer)[19] in an air-acetylene flame. The operating parameters for working elements were set as recommended by the manufacturer. Moreover, Cr(VI) ionic species remain unchanged within 24 hours; therefore, analysis of residual Cr(VI) was carried by overnight. Replication (minimum three replicates) was done in each experiment to ensure the reliability of Cr(VI) removal data. Equilibrium Cr(VI) adsorption for each adsorbent was determined in the range of 20–500 min. After that the effect of batch parameters like pH (2–7), temperature (30–50°C), initial Cr(VI) concentration (10–150 mg L^{-1}), adsorbent dose (0.5–3 g) and particle size (104–420 μm) on the Cr(VI) adsorption potential was optimized.

Adsorption capacity was calculated using the following mass balance equation:

$$q = \left(\frac{C_0 - C_f}{M}\right)V \quad (1)$$

q is the metal uptake (mg g^{-1}), C_o and C_f represent initial and final metal concentrations (mg L^{-1}), respectively, V represents the volume of synthetic solution used, and m indicates the mass of an adsorbent. The percentage removal of Cr(VI) was calculated by using the following equation

$$\% \text{ Removal} = \left(\frac{C_0 - C_f}{C_0}\right)100 \quad (2)$$

C_o and C_f indicates the initial and final metal concentrations (mg L^{-1}), respectively.

Characterization

The characterization of biomass was done using FTIR, SEM and EDX analyses. FTIR analysis of TS, EB and WCS was conducted to uncover the functional groups that could be involved in the Cr(VI) adsorption. All the dried adsorbents (before and after Cr(VI) adsorption) were transformed into pallets using KBr and then FTIR (Spectrum Two) spectra were recorded.

SEM analysis was used to study the surface morphology of adsorbents. In this method, the samples were placed on brass stubs using double-sided adhesive tape. SEM (JSM-5910) was used for taking SEM images at magnification range between X 250 and X 10,000. The photographs were collected at acceleration voltage of 5 kV and 20 kV using the secondary electron detector. EDX analysis (OXFORD made; UK model: INCA 200) of all adsorbents was carried out before and after Cr(VI) loading, and the adsorption of Cr(VI) was verified onto the surface of adsorbents.

Regeneration

For regeneration study, 0.05 g of each adsorbent (TS, EB and WCS) was treated with 50 mg L^{-1} of Cr(VI) solution at optimum time and temperatures. After filtration, the adsorbents were dried and treated with different eluents (potassium hydroxide, sulphuric acid, n hexane, nitric acid, acetic acid, ethanol, phosphoric acid, hydrochloric acid, acetone, citric acid, methanol, copper sulphate, acetonitrile, ethyl acetate, ferrous sulphate, sodium hydroxide and distilled water) of 0.1 M solutions. The mixtures were agitated at 220 rpm for 3 hrs. In all three saturated adsorbents, desorption with eluents was carried out at the temperature where less adsorption occurs so that may be higher desorption occurs at that temperature. The percentage (%) desorption was calculated by using the following equation 3.

$$\% \text{ desorption} = \left(\frac{\text{amount of Cr(VI) desorbed}}{\text{amount of Cr(VI) adsorbed}}\right) \times 100 \quad (3)$$

Statistical analysis

One-way analysis of variance (ANOVA) was conducted at a significance level of 0.01 to determine whether there was any statistically significant difference between results obtained from various biomasses which were used in the current study. Statistica 10 software was used. Significant difference ($p = 0.01$) among the biomass applied for Cr (VI) removal in the synthetic solution was evaluated.

RESULTS AND DISCUSSION

Potential lignocellulosic waste adsorbents for Cr(VI) removal

Cr(VI) removal potential of six waste adsorbents, i.e., maize cob (MC), sisal leaves (SL), peanut shells (PS), tobacco stalks (TS), white cedar stem (WCS) and eucalyptus bark (EB), was investigated in the batch experiments. The experimental conditions of adsorbent dose (0.05 g), Cr(VI) concentration (50 mg L^{-1}), solution pH (5.5), temperature (30°C), particle size (420 μm), agitation (220 rpm) and contact time (24 hours), were kept constants for all the adsorbents[20]. It was concluded

that the Cr(VI) removal was significantly ($p = 0.01$) high for EB (55%) than WCS (31%), TS (29%), PS (28%), SL (26%) and MC (23%) as shown in Figure 1. The presence of different functional groups (discussed in Figure 2) on the surface of EB, WCS and TS could be responsible for high Cr(VI) adsorption as compared to other studied adsorbents.

Three novel waste adsorbents namely TS, WCS (new for Cr(VI) removal studies) and EB were selected based on high treatment efficiency and availability in abundance in Pakistan. Removal % is higher than other many other studied adsorbents found in literature i.e., banana skin (25.5%), rice husk (25.2%), rice straw (26.3%), sawdust (19.9%) and walnut shell (24.6%)[21]. Influencing parameters of Cr(VI) adsorption were optimized in batch experiments.

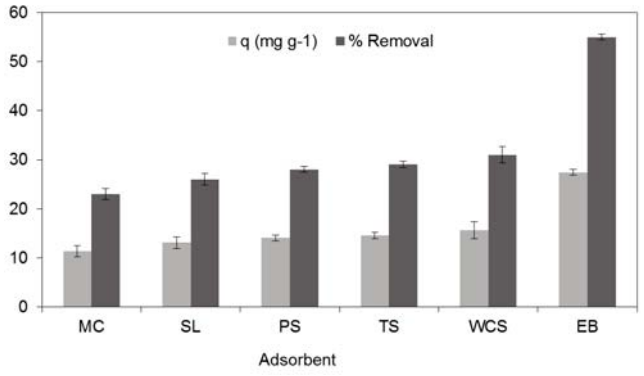

Figure 1. Screening of potential adsorbents for Cr(VI) removal: maize cob (MC), sisal leaves (SL), peanut shells (PS), tobacco stalks (TS), white cedar stem (WCS) and eucalyptus bark (EB)

FTIR analysis

FTIR spectra of TS before chromium adsorption shows peak at a 559 cm^{-1}, which can be assigned to O-H bending. While peaks at 560 cm^{-1} and 1021 cm^{-1} represent O-Si-O and C-O stretching respectively. The bands at 1375 cm^{-1} and 1598 cm^{-1} are characteristics of carbonyl group (C=O). Other peaks at 1684 cm^{-1}, 2845 cm^{-1}, 2913 cm^{-1} and 3370 cm^{-1} are indicators of hydrogen bonded -C=O stretching, CH_3, C-H and O-H groups respectively. In FTIR spectra of TS after adsorption of Cr(VI), Shift in peaks from 1598 cm^{-1} to 1578 cm^{-1}, 1684 cm^{-1} to 1679 cm^{-1} and 3370 cm^{-1} to 3378 cm^{-1} were observed in Figure 2, which confirms the involvement of C=O and O-H groups for Cr(VI) adsorption.

EB before Cr(VI) adsorption reflected spectral peaks at 1009 cm^{-1}, 1425 cm^{-1}, 1614 cm^{-1}, 1697 cm^{-1}, 2891 cm^{-1} and 3364 cm^{-1} which could be ascribed to Si-O bonding, C-H bending, C=N stretching, N-H vibration (out of plane bending), C-H aliphatic stretch and hydroxyl stretching respectively. Shift in three peaks was observed (Fig. 2), i.e., from 1697 cm^{-1} to 1704 cm^{-1}, 2891 to 2904 cm^{-1} and 3364–3390 cm^{-1}, which confirmed the involvement of N-H, C-H and OH functional groups during Cr(VI) adsorption.

WCS showed peaks at 556 cm^{-1} and 705 cm^{-1} which indicates the presence of metal oxide (Fe-O) and N-H wag vibrations due to secondary amines respectively. The peaks observed at 1018 cm^{-1}, 1376 cm^{-1} , 1590 cm^{-1}, 1680 cm^{-1}, 2840 cm^{-1}, 2909 cm^{-1} and 3369 cm^{-1} were associated with the C-O stretching, C-N stretching of aromatic amine group, C=C stretching, carbonyl stretching, methoxy group, C-H and N-H stretching vibrations respectively. Shift in two main peaks was observed from 705 cm^{-1} to 588 cm^{-1} and 1018 cm^{-1} to 1028 cm^{-1}. However, two peaks 1680 cm^{-1} and 2840 cm^{-1} disappeared after Cr(VI) adsorption as shown in Figure 2, which revealed the involvement of carbonyl and methoxy groups in the adsorption of chromium.

Literature shows that at low pH, protonation of the functional groups occurs, which results in strong electrostatic force of attraction between positively charged functional groups and negatively charged chromium ions; however, reverse was observed at high pH[20].

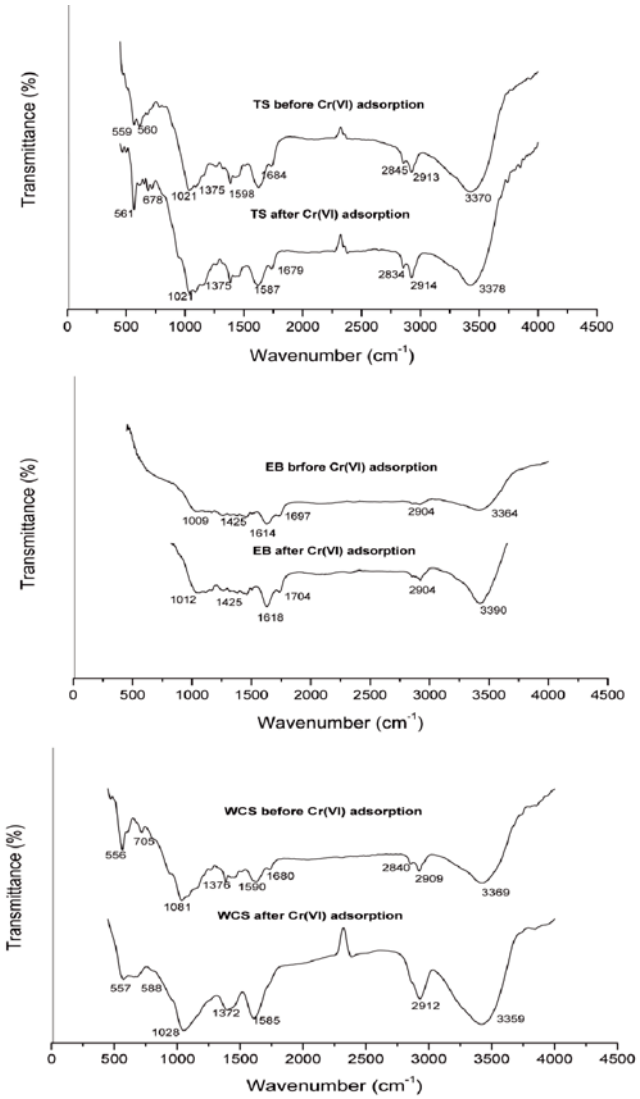

Figure 2. FTIR spectra of TS, EB and WCS before and after Cr(VI) adsorption

SEM and EDX analyses

Surface morphology of adsorbents can be studied by SEM. Figures 3, 4, 5 (a) showed that the surface of all adsorbents, i.e., TS, EB and WCS before Cr(VI) loading was porous and rough. While Figures 3, 5 (c, d) and Figure 4 (c) after Cr(VI) adsorption displayed the adsorption of Cr(VI) on adsorbent surface as the number of pores on the adsorbent surfaces were reduced or filled up[22]. EDX spectra was also taken to verify the Cr(VI) adsorption onto the surface of all adsorbents.

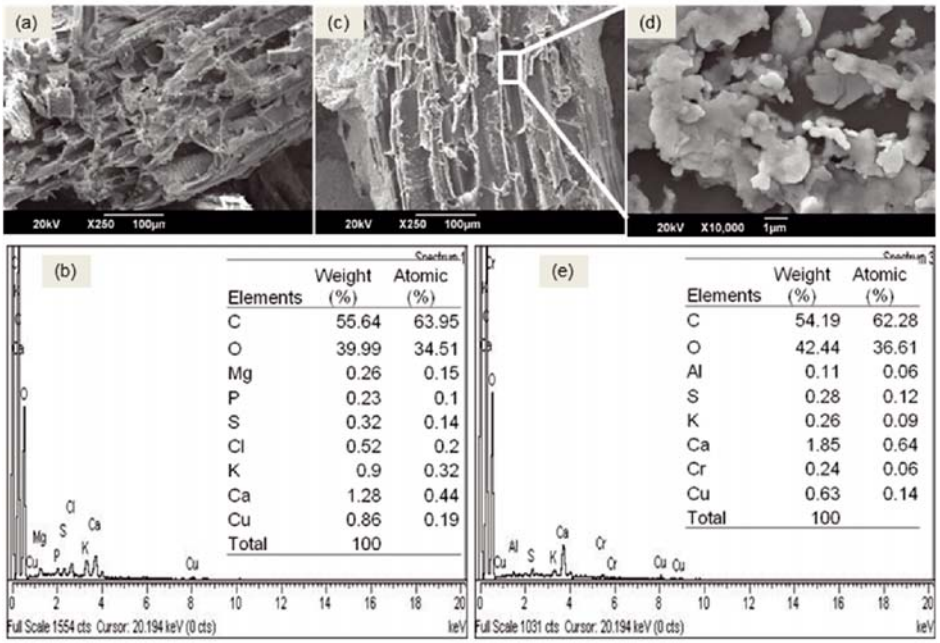

Figure 3. SEM and EDX images of TS before (a, b) and after (c, d, e) chromium ($HCrO_4^-$) ion adsorption

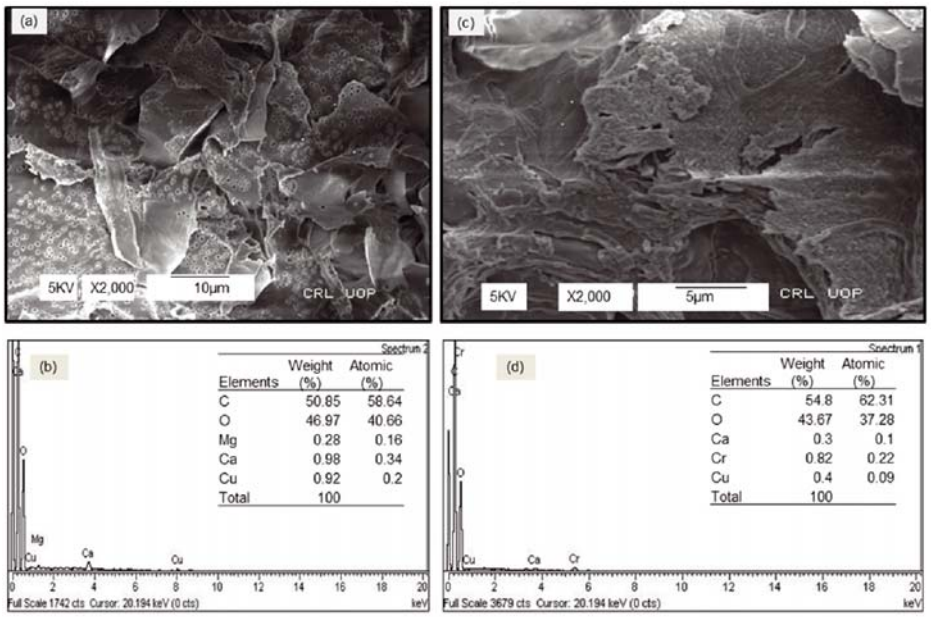

Figure 4. SEM and EDX images of EB before (a, b) and after (c, d) chromium ($HCrO_4^-$) ion adsorption

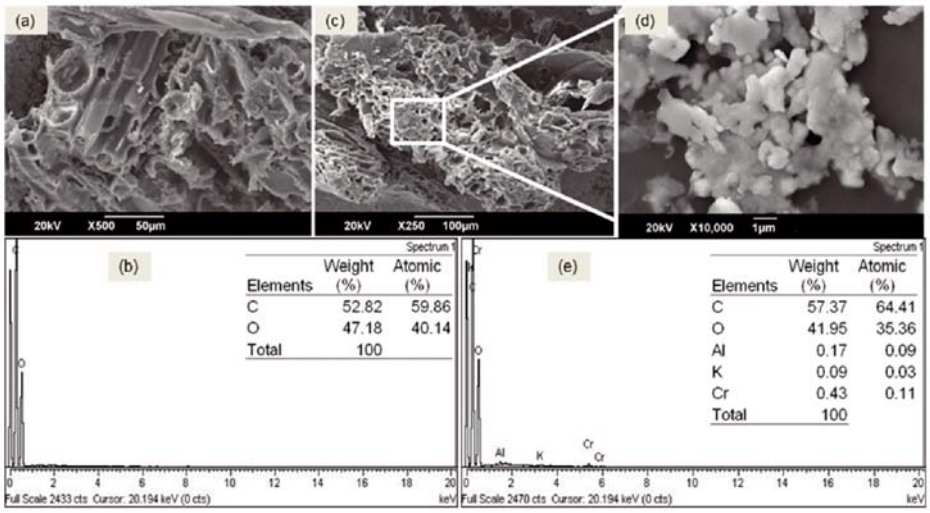

Figure 5. SEM and EDX images of WCS before (a, b) and after (c, d, e) chromium ($HCrO_4^-$) ion adsorption

It was evident from EDX spectra that the peak of Cr appeared at 5 to 6 KeV, which confirmed the adsorption of Cr(VI) by all the studied adsorbents (Figs. 3, 4(d), 5(e)). Similar peaks for Cr adsorption were observed for cellulose adsorbent at the same energy levels of 5 to 6 KeV[23]. In Figure 3, the biomass sampled for EDX measurements before and after Cr treatment are not necessarily the same. That is why, the disappearance of P, Cl, Mg in the biomass after Cr treatment is noticed.

Batch adsorption studies

Contact time

The effect of contact time was investigated on the Cr(VI) adsorption potential of TS, EB and WCS at variable time step. The equilibrium time was determined, in order to evaluate the shortest time required for Cr(VI) adsorption by each adsorbent (Fig. 6a). Figure 6a showed that initially adsorption capacity increased with time. Equilibrium adsorption of Cr(VI) was attained at 100 min for TS, 120 min for EB and 180 min for WCS. The initial sharp rise is associated with the availability of active sites, but adsorbent surface become saturated with Cr(VI)[24]. The effect of other parameters onto Cr(VI) adsorption was optimized at the aforesaid equilibrium time for each adsorbent.

pH

pH is an important parameter, which can affect metal speciation and surface charge of adsorbent. Relationship between pH and Cr (VI) adsorption was studied by carrying out batch experiments over different pH values from 2–7, while other parameters were kept constant. Results from the Figure 6b displayed that percentage removal and adsorption capacity were high, i.e., 28.5, 31.8, and 31 mg g^{-1} (57%, 63.66% and 62%) at pH 2 and decreased significantly ($p = 0.01$) at pH 7 i.e., 19.08, 19.85, 28.19 mg g^{-1} (38%, 39.69% and 56%) for TS, EB and WCS respectively. This is due to strong electrostatic attraction between protonated adsorbent surface and anionic chromium. There are many industries, which are releasing acidic wastewater containing chromium. Therefore they don't need addition of acids like electroplating industrial effluent having pH 1.65[26, 27]. However, decrease in Cr(VI) adsorption was observed at high pH. This is because of the increase in hydroxyl ions at the solid solution interface, which compete with chromate ions, in turn, the Cr(VI) adsorption is decreased onto the surface of adsorbents.

Adsorbent dose

Wastewater treatment at the industrial scale requires the optimization of adsorbent dosage because of its efficiency and economic importance. It was observed from Figue 6c that Cr(VI) removal efficiency increased

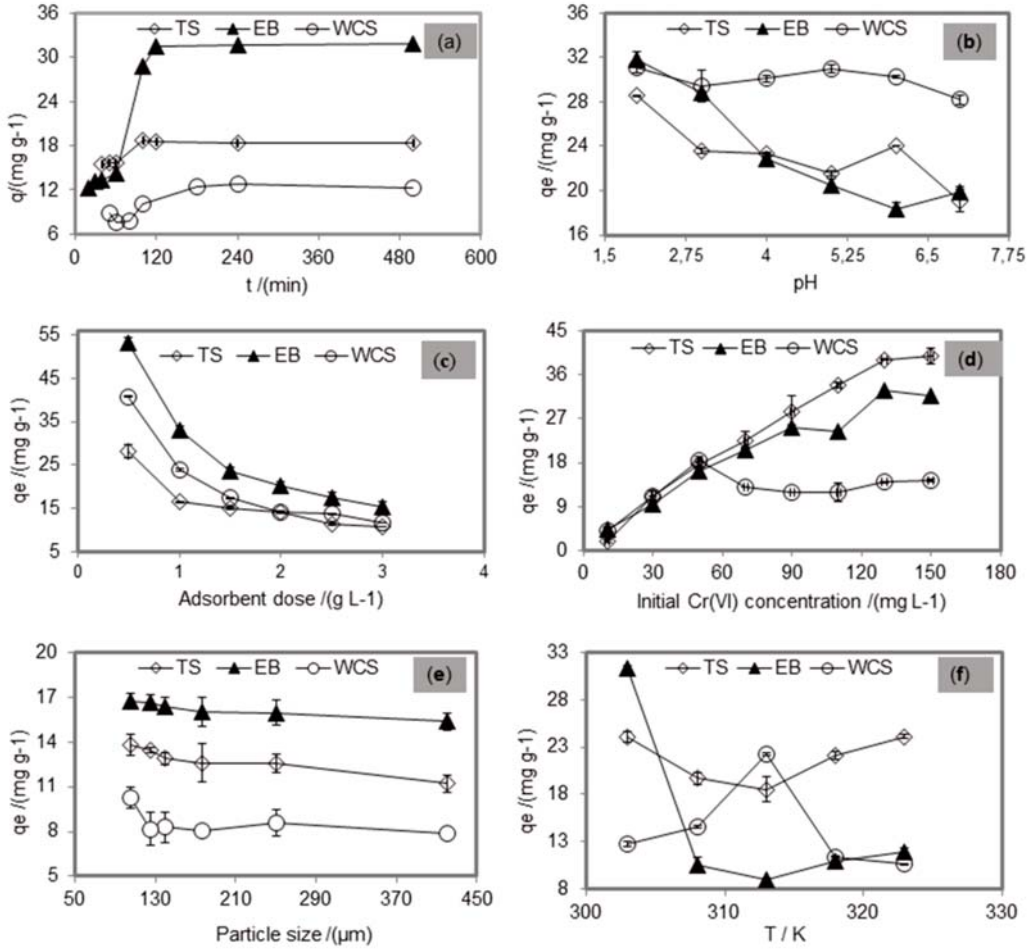

Figure 6. Cr(VI) removal capacity of TS, EB and WCS (a) contact time, (b) pH, (c) adsorbent dose, (d) initial metal concentration, (e) particle size (f) temperature. (Operating conditions except the variable parameter, initial Cr(VI) concentration 50 mg L^{-1}, pH 5.5, T 30°C, adsorbent dose 0.05 g L^{-1}, agitation speed 220 rpm, particle size 420 μm, equilibrium time for TS (100 minutes), EB (120 minutes), WCS (180 minutes)

significantly ($p = 0.01$) from 43.69% to 78.47% upon the increase of TS adsorbent dose from 0.5 g L^{-1} to 3 g L^{-1}. Similarly respective Cr(V) adsorption efficiencies for EB and WCS adsorbents also increased significantly 53.28% to 92.79% and 18.5% to 76.64%, respectively with the increase of adsorbent dose. This can be ascribed to increase in active adsorption sites, which is reflected with more Cr(VI) adsorption onto the adsorbent's surface. Conversely, adsorption capacities decreased significantly ($p = 0.01$) from 28 mg g^{-1} to 10.7 mg g^{-1}, 53.25 mg g^{-1} to 15.46 mg g^{-1} and 40.75 mg g^{-1} to 11.6 mg g^{-1} for TS, EB and WCS respectively. This can be attributed to partial overlapping or aggregation at higher adsorbent dose[18].

Initial metal concentration

Figure 6d showed that Cr(VI) adsorption capacity increased significantly ($p = 0.01$) for TS, EB and WCS from 1.89 to 39.8, 4.26 to 31.78 mg g^{-1} and 4 to 14 mg g^{-1}, respectively, by increasing the initial metal concentration from 10 to 150 mg g^{-1}. However, percentage removal of Cr(VI) decreased from 36.87 to 26.5%, 42.6 to 21% and 41.46 to 9.5% for TS, EB and WCS respectively. At lower adsorbate concentration, the available active adsorbent sites are high, therefore, the adsorption is independent of adsorbate concentration. On the other hand, when Cr(VI) concentration is high, the available active adsorbent sites per unit mass become less, which reduces percentage adsorption, showing that adsorption depends on the adsorbate concentration.

Particle size

The effect of particle size onto Cr(VI) adsorption potential of adsorbents was investigated by varying the particle size from 420–105 microns. Results show (Fig. 6e) that both adsorption capacity and percentage removal of TS, EB and WCS for Cr(VI) increased significantly ($p = 0.01$) from 11 to 13.79 mg g^{-1} (22.43 to 27.59%), 15.35 to 16.68 mg g^{-1} (30.7 to 33.37%) and 7.86 to 10.24 mg g^{-1} (15.7 to 20.48%), respectively. Size reduction of adsorbents results in high surface area, and active sites of absorbent are exposed to adsorbate. This results in better interaction between adsorbate and active sites, which promote the adsorption capacity of adsorbents.

Temperature and Thermodynamic studies

The mechanism of adsorption, i.e., physisorption or chemisorption, can be an important indicator to explain the level and type of interaction between adsorbate and adsorbent. Effect of temperature onto Cr(VI) adsorption capacity of all adsorbents was explored at two temperature ranges T_1 (303–313 K) and T_2 (313–323 K). Thermodynamic parameters were also evaluated to identify the nature of the adsorption process.

The distribution coefficient K_d was calculated from Eq. (4).

$$K_d = \frac{q_e}{C_e} \tag{4}$$

q_e (mg g^{-1}) is the solid phase concentration and C_e (mg L^{-1}) is the liquid phase concentration at equilibrium. This was further used in Van't Hoff plot. Change in enthalpy and entropy were calculated from Van't Hoff plot by using Eq. (5).

$$\ln K_d = \frac{\Delta S}{R} - \frac{\Delta H}{RT} \tag{5}$$

ΔH (kJ mol^{-1}) is the change in standard enthalpy, ΔS is change in standard entropy (kJ mol^{-1}), K_d is the distribution coefficient of adsorption (q_e/C_e), R is universal gas constant (8.314 J mol^{-1} K^{-1}) and T is the temperature (K). Change in Gibbs free energy (ΔG (kJ mol^{-1}) was determined using the Eq. (6).

$$\Delta G = \Delta H - T\Delta S \tag{6}$$

At T1, TS and EB reflected decrease (24 to 18.5 mg g^{-1} and 31 to 9 mg/g, respectively) in Cr(VI) adsorption (Fig. 6f) and values of ΔH and ΔS for TS and EB are also negative, which indicates exothermic nature (physisorption), as well as less randomness at the solid-solution interface during the adsorption of Cr(VI) onto the surface of studied adsorbents. For both TS and EB, enthalpy is less than zero, which signify that reaction is favorable for enthalpy, but unfavorable for entropy ($\Delta S<0$). This reveals that Cr(VI) adsorption is not controlled by the entropy of the system and the surface active sties of both biomasses remain stable. The value of ΔG is greater than zero which confirms the non-spontaneous nature of adsorption for all studied adsorbents. However, in case of WCS, increase in adsorption capacity from 12.7 to 22 mg g^{-1} (25.5 to 44%) was observed (Fig. 6f), similarly ΔH and ΔS are positive, which confirms endothermic process (chemisorptions) and increased randomness at the solid-solution interface during adsorption of Cr(VI) onto the surface of WCS. While $\Delta H> 0$ in WCS which is an indication of unfavorable reaction, however, ΔS is also greater than zero which confirms entropy controlled favorable Cr(VI) adsorption process and $\Delta G>0$ shows that free energy increases with an increase in time.

This is contrary to T1 range, where decrease in Cr(VI) removal (22 mg g^{-1} to 10.6 mg g) was observed (Fig. 6f) and ΔH value for WCS is also negative ($\Delta H<0$) which indicates the exothermic and favorable adsorption process and ΔS ($\Delta S<0$) is positive which is an indication of increased randomness and unfavorable adsorption of Cr(VI) onto the surface of WCS should be corrected as This is contrary to WCS, where decrease in Cr(VI) removal (22 mg g^{-1} to 10.6 mg g) was observed (Fig. 6f) and ΔH value for WCS is negative ($\Delta H<0$) which indicates the exothermic and favorable adsorption process and ΔS ($\Delta S<0$) is also negative which is an indication

Table 1. Thermodynamics parameters of Cr(VI) adsorption onto TS, EB and WCS adsorbent at temperature range of T1 (303–313K) and T2 (313–323K)

Adsorbents	Temperature [K]	ΔH [KJ mol^{-1}]	ΔS [KJ mol^{-1}]	ΔG [kJ mol^{-1}]		
TS	T1	−34.24	−0.11	0.32	0.89	1.46
	T2	40.04	0.12	1.34	0.72	0.10
EB	T1	−159.65	−0.52	0.72	1.90	4.52
	T2	30.34	0.09	3.89	3.47	3.05
WCS	T1	78.89	0.25	2.66	1.41	0.149
	T2	−125.12	−0.40	0.32	2.32	4.33

of less randomness and favorable adsorption of Cr(VI) onto the surface of WCS.

Isotherm models

It is often useful to employ the mathematical models to compare the metal adsorption strength and to design adsorption process effectively. Most frequently used isotherms like Langmuir, Freundlich and Dubinin-Radushkevich were applied for the analysis of experimental data.

Langmuir isotherm model

According to Langmuir (1918), adsorption takes place by monolayer adsorption on the homogeneous active sites onto the surface of adsorbents and there is negligible interaction between adsorbed molecules. Moreover, there is no transmigration of Cr(VI) ions onto the surface of adsorbent. The Langmuir isotherm equation can be written as:

$$q_e = (q_{max} K_{ads} C_e) / (1 + K_{ads} C_e) \quad (7)$$

q_e is the amount of Cr(VI) adsorbed at equilibrium per g of adsorbent, q_{max} is the maximum adsorption capacity of adsorbent, C_e is adsorbate concentration in solution and K_{ads} is Equilibrium constant.

The linear form of equation 7 is:

$$\frac{1}{q_e} = \frac{1}{q_{max}} + \left(\frac{1}{q_{max} K_{ads}}\right) \frac{1}{C_e} \quad (8)$$

$$R_L = \frac{1}{1 + (q_{max} \times b) C_0} \quad (9)$$

Value of RL indicates isotherm shape to be linear (RL = 1), favorable (0<RL<1), unfavorable (RL>1) and irreversible adsorption (RL = 0). Value of R_L in all three adsorbents TS (0.602702), WCS (0.136557) and EB (0.345103) shows that these adsorbents are suitable for Cr(VI) adsorption. This model shows (Fig. 7a, Table 2) best fitting to the adsorption data of EB (R^2 = 0.999) than TS (R^2 = 0.9978) and WCS (R^2 = 0.9937). It suggests that the Cr(VI) adsorption almost reach saturation onto EB adsorbent, and ion-exchange reactions produce the favorable adsorption isotherms. Moreover, K_{ads} value was high for EB adsorbent, which suggested that EB hold the strength to retain Cr(VI) even when the residual Cr(VI) concentrations were low. TS and EB showed maximum monolayer Langmuir adsorption capacity of 42.08 mg g^{-1} and 43 mg g^{-1} which is higher than the values reported recently in non-modified form of adsorbent[25].

Freundlich isotherm model

Freundlich assumes that adsorption is a heterogeneous process in which several energies are involved. This model is used to estimate the adsorption intensity of the adsorbent towards the pollutant. Freundlich isotherm equation is as follows:

$$q_e = K_F C_e^{1/n} \quad (10)$$

Both K_f (adsorption capacity) and 1/n (adsorption intensity) are Freundlich constants. High K_f value shows high adsorption capacity, therefore, it is concluded that WCS have high adsorption capacity as compared to EB and TS (Table 2). Moreover, 1/n measures adsorption

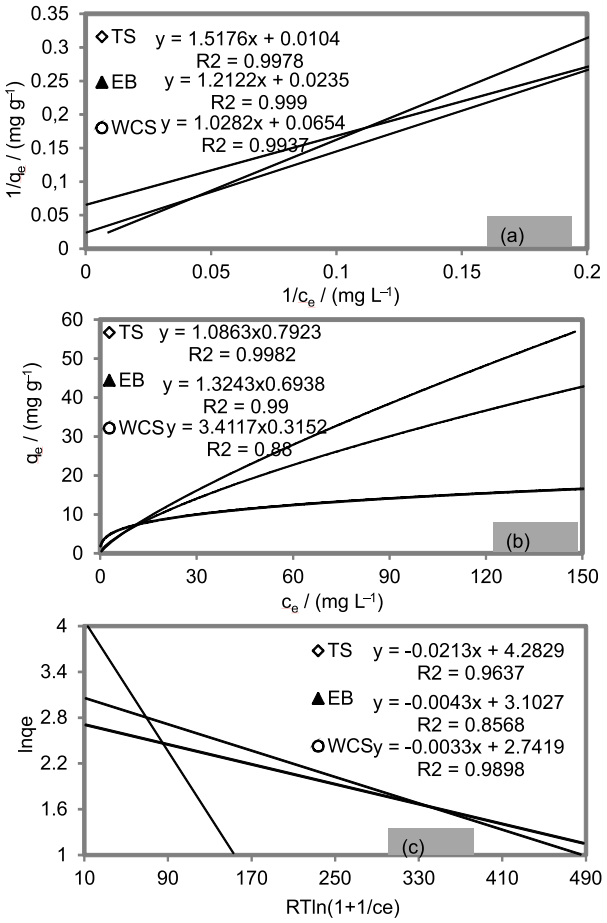

Figure 7. Plot of (a) Langmuir (b) Freundlich and (c) Dubinin-Radushkevich isotherms

Table 2. Langmuir, Freundlich, and D-R parameters for Cr(VI) adsorption by TS, EB and WCS

Models	Parameters	Value [TS]	Value [EB]	Value [WCS]
Langmuir isotherms	q_{exp} [mg g^{-1}]	39.8	31.78	14.3
	q_{max} [mg g^{-1}]	42.08	43.48	15.39
	K_{ads} [L mg^{-1}]	0.007	0.019	0.063
	R^2	0.9978	0.999	0.9937
Freundlich isotherm	q_{max}[mg g^{-1}]	37.56	45.14	54.59
	1/n	0.792	0.693	0.315
	N	1.27	1.44	3.17
	KF [L g^{-1}]	1.09	1.32	3.41
	R^2	0.9982	0.99	0.88
Dubinin-Radushkevich isotherm	q_{DR} [mol g^{-1}]	51.63	22.24	15.60
	β [mol J^{-1}]^2	0.006	0.002	0.0015
	E [KJ mol^{-1}]	9.13	15.81	18.26
	R^2	0.963	0.856	0.989

intensity or surface heterogeneity, if value of 1/n is more closer to zero it shows more heterogeneity of adsorbent. Results show more heterogeneity of WCS as compared to EB and TS adsorbents. If value of 1/n lies between 0 and 1, then it confirms a favorable adsorption. Value of 1/n for TS, EB and WCS represent favorable adsorption (Table 1). Correlation coefficient (R^2) value for all three adsorbents were in the order of EB (0.99) > TS (0.9982) > WCS (0.88) (Fig. 7b). It concludes that Cr(VI) adsorption can be increased with increasing equilibrium adsorbate concentration.

Dubinin-Radushkevich (D-R) isotherm

D-R isotherm is used to determine the physical or chemical nature of adsorption. It is generally expressed as:

$$\ln q_e = \ln q_{DR} - \beta\varepsilon^2 \quad (11)$$

Here q_{DR} is the theoretical monolayer sorption capacity (mol g^{-1}), β is the constant of sorption energy (mol^2J^{-2}), β is Polanyi potential, *T* is the solution temperature (K) and *R* is the gas constant (8.314 J mol^{-1} K^{-1}).

$$\varepsilon = RT \ln\left(1 + \frac{1}{C_e}\right) \quad (12)$$

E is the average or apparent energy of adsorption and can by using the following formula:

$$E = \frac{1}{\sqrt{-2\beta}} \quad (13)$$

The value of E (kJ · mol^{-1}) is used to estimate the adsorption mechanism. If the value of E is between 8 and 16 kJ · mol^{-1}, the adsorption is chemisorption, and if E is less than 8 kJ · mol^{-1}, the adsorption follows physical mechanism. From the experimental data, it was observed that the value of E (mean free energy) for TS was 9.12 kJ · mol^{-1}, which confirms the chemisorption nature of adsorption. Similarly mean free energy (E) for EB and WCS was 15.81 and 18.25 kJ · mol^{-1} respectively, which indicates that adsorption of Cr(VI) onto the surfaces of WCS and EB follows chemisorption. Regression coefficient (R^2) value for WCS, TS and EB is 0.989, 0.963 and 0.856 respectively (Fig. 7c). Higher the value of q_{DR} higher will be the adsorption capacity, therefore it is confirmed from q_{DR} that TS have high adsorption capacity as compared to WCS and EB (Table 2).

Pseudo second-order kinetic model

Pseudo-second order kinetic model was used to analyze the experimental data and to investigate mechanism and rate of adsorption of Cr(VI) onto the surface of TS, EB and WCS adsorbents.

According to this model, chemisorption is the rate limiting step in adsorption and involves exchange/sharing of electrons between biomass and pollutant. This model is generally expressed as follows:

$$\frac{t}{q_t} = \frac{1}{k_2 q_e^2} + \frac{1}{q_e} t \quad (14)$$

K_2 (g mg^{-1} min^{-1}) is pseudo-second order rate constant, q_e(mg g^{-1}) represents adsorption capacity, q_t is the amount of adsorbed Cr(VI) at time *t* (min), h (mg · g^{-1} hr^{-1}) is the initial adsorption rate.Initial adsorption rate ($h = k_2 q_e^2$), q_e (mg g^{-1}) and K_2 (g mg^{-1} min^{-1}) were calculated from the slope and intercept of the plot t/q_t versus t (Fig. 8a, b).

q_{exp} for TS adsorbent showed a good agreement with the q_{cal} value at both 50 and 70 mg L^{-1} concentration of Cr(VI) (Table 3). K_2 (g mg^{-1} min^{-1}) increases with increase in concentration from 50 (0.002413) to 70 mg L^{-1} (0.0033), similarly *h* increases from 1.14 to 1.2 with increase in Cr(VI) concentration (Table 3). Regression coefficient (R^2) for TS at 50 mg L^{-1} is greater than 70 mg L^{-1} (0.960), it means that pseudo-second order kinetic shows better fit to adsorption data at low initial Cr(VI) concentration. While for both EB and WCS, values of K_2 and *h* decrease as the Cr(VI) concentration increases from 50 to 70 mg L^{-1}. Contrary to this, regression coefficient (R^2) increases from 0.992 to 0.993 and 0.958 to 0.983 for EB and WCS respectively. It suggests that pseudo second order model show good fit to Cr(VI) adsorption for EB and WCS adsorbents. Moreover, based on regression coefficient (R^2) values, it can be

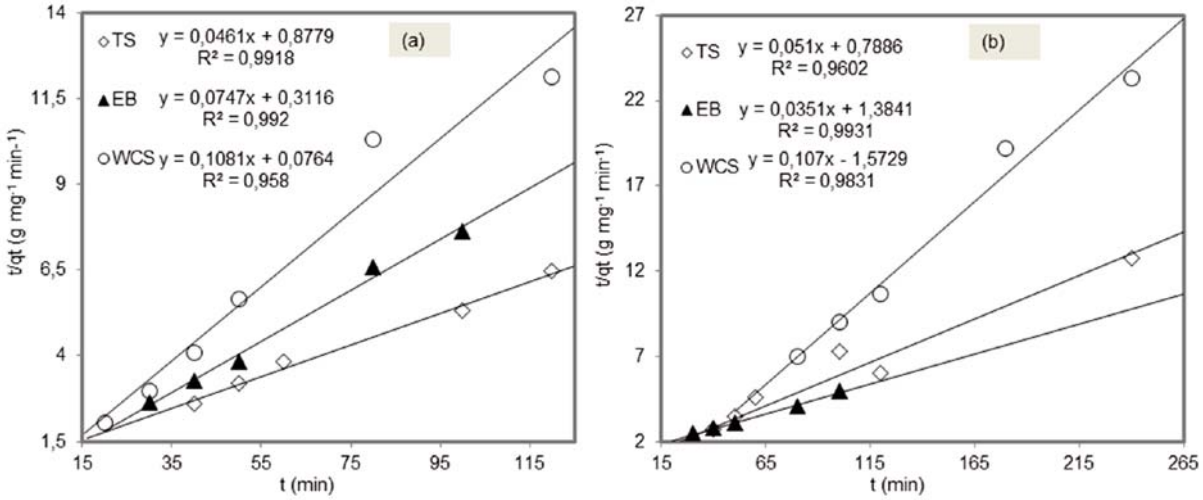

Figure 8. Pseudo-second order plot for Cr(VI) adsorption onto TS, EB and WCS at initial concentration of 50 mg L^{-1} (a) and 70 mg L^{-1} (b)

Table 3. Pseudo-second order constants for TS, EB and WCS at Cr(VI) concentration of 50 mg L^{-1} and 70 mg L^{-1}

Adsorbents	Cr(VI) Conc. [mg L^{-1}]	q_{exp}. [mg g^{-1}]	K_2 [g mg^{-1} min^{-1}]	q_{cal} [mg g^{-1}]	*h* [mg g^{-1} min^{-1}]	R^2
TS	50	21.66	0.002413	21.739	1.1402	0.991
	70	19.83	0.0033	19.607	1.269	0.960
EB	50	13.083	0.0176	13.51	3.215	0.992
	70	20.016	0.00088	28.571	0.722	0.993
WCS	50	13.43	0.1535	9.259	13.157	0.958
	70	15.71	0.00728	9.3457	0.636	0.983

concluded that chemisorption is the rate limiting step, and adsorption dominates rather than reduction of Cr(VI). All the studied adsorbents, based on regression coefficient, display the following order EB > TS > WCS at 50 mg L^{-1} and EB > WCS> TS at 70 mg L^{-1} solution concentration of Cr(VI).

Regeneration studies

EB showed high desorption of 28% with sulphuric acid followed by TS 27% with citric acid and WCS 26% with nitric acid (Fig. 9). This small desorption showed that chemisorption is the binding mechanism in case of all three adsorbents. So it is difficult to regenerate these adsorbents even with acids and base. However these adsorbents are available in bulk as the waste materials, therefore, they can be used without considering the regeneration in the developing country scenario like Pakistan.

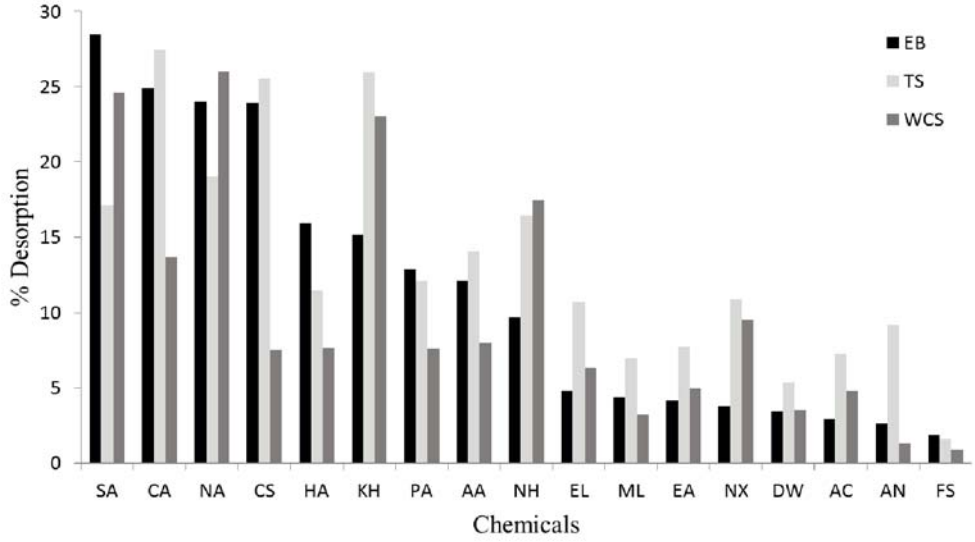

Figure 9. Regeneration of Cr(VI) from EB, TS and WCS using 0.1 M solutions of sulphuric acid (SA), citric acid (CA), nitric acid (NA), copper sulphate (CS), hydrochloric acid (HA), potassium hydroxide (KH), phosphoric acid (PA), acetic acid (AA), sodium hydroxide (NH), ethanol (EL), methanol (ML), ethyl acetate (EA), n-hexane (NX), deionized water (DW), acetone (AC), acetonitrile (AN) and ferrous sulphate (FS)

CONCLUSIONS

Tobacco stalks (TS), eucalyptus bark (EB) and white cedar stem (WCS) were explored for Cr(VI) adsorption potential. EDX confirms the adsorption of Cr(VI) in all three adsorbents. Study shows that at pH 2, the maximum Cr(VI) adsorption was observed for EB followed by TS and WCS respectively. Cr(VI) adsorption by TS, EB and WCS obey the pseudo-second order kinetics, which shows that chemisorptions is the rate limiting step. This is also confirmed through D-R isotherms where value of *E* is greater than 8 for each adsorbent. It was found that Freundlich (R^2 = 0.998) isotherm best fitted to the equilibrium data of TS, reflecting the multilayer adsorption. Langmuir (R^2 = 0.999) isotherm best fitted to the experimental data of both EB and WCS indicating monolayer coverage for EB and WCS adsorbents. Regression coefficient values show that EB follows pseudo-second order better than TS and WCS at both concentrations of 50 mg L^{-1} and 70 mg L^{-1}. Results of all parameters reflects that among all studied adsorbents, EB have highest adsorption capacity at optimum conditions of time (120 min), pH (2), adsorbent dose (3 g L^{-1}), particle size (105 micron) and temperature of 303 K. Therefore it can be concluded that EB can be a good choice for treatment of Cr(VI) than TS and WCS.

ACKNOWLEDGEMENTS

The authors extend their thanks to the Higher Education Commission of Pakistan, providing funding for a research project (20–1915/R&D/10/[5253]).

LITERATURE CITED

1. Chowdhury, M., Mostafa, M., Biswas, T.K. & Saha, A.K. 2013. Treatment of leather industrial effluents by filtration and coagulation processes. *Water Res. Ind.* 3, 11–22. DOI: 10.1016/j.wri.2013.05.002.

2. Honnannavar, S.M. & Hosamani, S.R. 2014. Comparison of activated and inactivated coconut husk as an adsorbent for removal of hexavalent chromium from wastewater. *J. Chem. Pharm. Res.* 6, 2628–2633. http://jocpr.com/vol6-iss6-2014/JCPR-2014-6-6-2628-2633.pdf

3. Kerger, B.D., Paustenbach, D.J., Corbett, G.E. & Finley, B.L. 1996. Absorption and elimination of trivalent and hexavalent chromium in humans following ingestion of a bolus dose in drinking water. *Toxicol. Appl. Pharm.* 141, 145–158. http://dx.doi.org/10.1016/S0041-008X(96)80020-2

4. Gomez, V. & Callao, M. 2006. Chromium determination and speciation since 2000. *TrAC Trends Anal. Chem.* 25, 1006–1015. DOI: 10. 1016/j.trac.2006.06.010.

5. Barrera-Díaz, C.E., Lugo-Lugo, V. & Bilyeu, B. 2012. A review of chemical, electrochemical and biological methods for aqueous Cr (VI) reduction. *J. Hazard. Mater.* 223, 1–12. DOI: 10. 1016/j.jhazmat.2012.04.054.

6. Chen, D., Zhang, J. & Chen, J. 2010. Adsorption of methyl tert-butyl ether using granular activated carbon: Equilibrium and kinetic analysis. *Int. J. Environ. Sci. Tech.* 7, 235–242. DOI: 10.1007/BF03326133.

7. Kennedy, L.J., Vijaya, J.J. & Sekaran, G. 2004. Effect of two-stage process on the preparation and characterization of porous carbon composite from rice husk by phosphoric acid activation. *Ind. Eng. Chem. Res.* 43, 1832–1838. DOI: 10.1021/ie034093f.

8. Sivakumar, D. 2013. Experimental and analytical model studies on leachate volume computation from solid waste. *Int. J. Environ. Sci. Technol.* 10, 903–916. DOI: 10.1007/s13762-012-0083–1.

9. Akbal, F. & Camcı, S. 2012. Treatment of metal plating wastewater by electrocoagulation. *Environ. Prog. Sustain. Energy.* 31, 340–350. DOI: 10.1002/ep.10546.

10. Kurniawan, T.A., Chan, G.Y.S., Lo, W.H. & Babel, S. 2006. Physico–chemical treatment techniques for wastewater laden with heavy metals. *Chem. Eng. J.* 118, 83–98. DOI: 10.1016/j.cej.2006.01.015.

11. Mohan, D., Rajput, S., Singh, V.K., Steele, P.H. & Pittman, C.U. 2011. Modeling and evaluation of chromium remediation from water using low cost bio-char, a green adsorbent. *J. Hazard. Mater.* 188, 319–333. DOI: 10. 1016/j.jhazmat.2011.01.127.

12. Dave, P.N., Pandey, N. & Thomas, H. 2012. Adsorption of Cr (VI) from aqueous solutions on tea waste and coconut husk. *Indian J. Chem. Technol.* 19, 111–117.

13. Jain, R.N., Patil, S. & Lal, D. 2014. Adsorption of Cr (VI) from aqueous environment using neem leaves powder. *Int. J. Res. Eng. Tech.* 3. http://esatjournals.net/ijret/2014v03/i21/IJRET20140321007.pdf

14. Mutongo, F., Kuipa, O. & Kuipa, P.K. 2014. Removal of Cr (VI) from aqueous solutions using powder of potato peelings as a low cost sorbent. *Bioinor. Chem. Appl.* 2014. DOI: 10.1155/2014/973153.

15. Gao, H., Liu, Y., Zeng, G., Xu, W., Li, T. and Xia, W. 2008. Characterization of Cr(VI) removal from aqueous solutions by a surplus agricultural waste-rice straw. *J. Hazard. Mater.* 150, 446–452. DOI: 10.1016/j.jhazmat.2007.04.126.

16. Ahmad, R., Rao, R.A.K. & Masood, M.M. 2005. Removal and recovery of Cr (VI) from synthetic and industrial wastewater using bark of *Pinus roxburghii* as an adsorbent. *Water Qual. Res. J. Can.* 40, 462–468.

17. Ahalya, N.K., R.D. & Ramachandra, T.V. 2005. Biosorption of chromium (VI) from aqueous solutions by the husk of Bengal gram (*Cicer arientinum*). *Electron. J. Biotech.* 8, 258–264. DOI: 10.2225/vol8-issue3-fulltext–10.

18. Garg, U.K., Kaur, M., Garg, V. & Sud, D. 2007. Removal of hexavalent chromium from aqueous solution by agricultural waste biomass. *J. Hazard. Mater.* 140, 60–68. DOI: 10.1016/j.jhazmat.2006.06.056.

19. Lu, M., Guan, X.H., Xu, X.H. & Wei, D.Z. 2013. Characteristic and mechanism of Cr(VI) adsorption by ammonium sulfamate-bacterial cellulose in aqueous solutions. *Chinese Chem. Lett.* 24, 253–256. DOI: /10.1016/j.cclet.2013.01.034

20. Haroon, H., Ashfaq, T., Gardazi, S.M.H., Sherazi, T.A., Ali, M., Rashid, N. & Bilal, M. 2016. Equilibrium kinetic and thermodynamic studies of Cr(VI) adsorption onto a novel adsorbent of Eucalyptus camaldulensis waste: Batch and column reactors. *Korean J. Chem. Eng.* 33, 2898–2907. DOI: 10.1007/s11814-016-0160-0.

21. Park, D., Lim, Seong-Rin., Yun, Yeoung-Sang., Park, J. M. 2007. Reliable evidences that the removal mechanism of hexavalent chromium by natural biomaterials is adsorption-coupled reduction. *Chemosphere* 70, 298–305. DOI:10.1016/j.chemosphere.2007.06.007.

22. Nharingo, T., Moyo, M. & Mahamadi, C. 2016. Kinetics and Equilibrium Studies on the Biosorption of Cr(VI) by *Vigna Subterranean* (L.) *Verdc* Hull. *Int. J. Environ. Res.* 10, 85–96.

23. Lin, C., Qiao, S., Luo, W., Liu, Y., Liu, D., Li, X. & Liu, M., 2014. Thermodynamics, Kinetics, and Regeneration Studies for Adsorption of Cr (VI) from Aqueous Solutions using Modified Cellulose as Adsorbent. *BioResources* 9, 6998–7017. DOI: 10.15376/biores.9.4. 6998-7017.

24. Aliabadi, M., Khazaei, I., Fakhraee, H. & Mousavian, M. 2012. Hexavalent chromium removal from aqueous solutions by using low-cost biological wastes: equilibrium and kinetic studies. *Int. J. Environ. Sci. Tech.* 9, 319–326. DOI: 10.1007/s13762-012-0045-7.

25. Tadesse, B., Teju, E. & Megersa, N. 2015. The Teff straw: a novel low-cost adsorbent for quantitative removal of Cr (VI) from contaminated aqueous samples. *Desalin. Water Treat.* 56, 2925–2936. DOI:10.1080/19443994.2014.968214.

26. Singh, V., Ram, C. & Kumar. A. 2016. Physico-chemical characterization of electroplating industrial effluents of Chandigarh and Haryana Region. J. Civil. Environ. Eng. 6, 2–6. DOI: 10.4172/2165-784X.1000237

27. Verma, S.K., Khandegar, V. & Saroha, Anil-K. 2013. Removal of chromium from electroplating industry effluent using electrocoagulation. J. Hazard. Toxic Radioact. Waste. 17, 146–152. DOI: 10.1061/(ASCE)HZ.2153-5515.0000170.